PROJECT REPORT

On

SYNTHESIS, CHARACTERIZATION AND APPLICATION STUDIES OF ZnO-Mo_2TiC_2 NANOHYBRID

Submitted by

Amritha Lakshmi M S (AB23CHE029)

In partial fulfillment for the award of the

Bachelor's Degree in Chemistry

DEPARTMENT OF CHEMISTRY AND CENTRE FOR RESEARCH

ST. TERESA'S COLLEGE (AUTONOMOUS)
ERNAKULAM

2025-2026

DEPARTMENT OF CHEMISTRY AND CENTRE FOR RESEARCH

ST. TERESA'S COLLEGE (AUTONOMOUS)

ERNAKULAM

B.Sc. CHEMISTRY PROJECT REPORT

Name : **Amritha Lakshmi M S**
Register Number : **AB23CHE029**
Year of Work : **2025-2026**

This is to certify that the project "**Synthesis, Characterization and Application Studies of ZnO-Mo_2TiC_2 Nanohybrid**" is the work done by **Amritha Lakshmi M S**

6/3/26

Dr. Saritha Chandran A.
Head of the Department

Dr. Nisha T P
Staff-member in charge

Submitted to the Examination of Bachelor's Degree in Chemistry

Date: 10/04/2026

Examiners: SENJU. D. VASSYKUTTY

:

DEPARTMENT OF CHEMISTRY AND CENTRE FOR RESEARCH

ST. TERESA'S COLLEGE (AUTONOMOUS)

ERNAKULAM

CERTIFICATE

This is to certify that the project work entitled "**Synthesis, Characterization and Application Studies of ZnO-Mo_2TiC_2 Nanohybrid**" is the work done by **Amritha Lakshmi MS** under my guidance in the partial fulfilment of the award of the Degree of Bachelor of Science in Chemistry at St. Teresa's College (Autonomous), Ernakulam affiliated to Mahatma Gandhi University, Kottayam.

6/3/26

Dr. Nisha T P
Assistant Professor,
Department of Chemistry and Centre for Research

DECLARATION

I hereby declare that the project work entitled "**Synthesis, Characterization and Application Studies of ZnO-Mo_2TiC_2 Nanohybrid**" submitted to Department of Chemistry and Centre for Research, St. Teresa's College (Autonomous) affiliated to Mahatma Gandhi University, Kottayam, is a record of an original work done by me under the guidance of **Dr. Nisha T P,** Assistant Professor, Department of Chemistry and Centre for Research, St. Teresa's College (Autonomous), Ernakulam, and this project work is submitted in the partial fulfilment of the requirements for the award of the Degree of Bachelor of Science in Chemistry.

Amritha Lakshmi MS

Acknowledgements

We express our sincere gratitude to Almighty God for bestowing us with the strength, guidance, and perseverance to complete this project successfully.

We extend our heartfelt thanks to our project supervisor, Dr. Nisha T. P., Assistant Professor, Department of Chemistry and Centre for Research, St. Teresa's College (Autonomous), Ernakulam, for her constant guidance, valuable suggestions, and unwavering support throughout the course of this work.

We are deeply grateful to Dr. Saritha Chandran A., Head of the Department, Department of Chemistry and Centre for Research, St. Teresa's College (Autonomous), Ernakulam, for her encouragement and for providing a conducive academic environment. We sincerely thank Dr. Anu Joseph, Principal, St. Teresa's College (Autonomous), Ernakulam, for her administrative support and motivation. We also extend our gratitude to Rev. Sr. Nilima, Manager, and the Directors Rev. Sr. Francis Ann and Rev. Sr. Tessa CSST, St. Teresa's College (Autonomous), Ernakulam, for their constant support and encouragement.

We express our sincere appreciation to all the teachers of the Department of Chemistry and Centre for Research for their guidance and cooperation. We also thank the non-teaching staff for providing all the necessary laboratory facilities and chemicals required for carrying out our project work.

We gratefully acknowledge Teresian Instrumentation and Consultancy Centre (TICC), St. Teresa's College (Autonomous), Ernakulam, for their support. We also extend our sincere thanks to Sophisticated Test and Instrumentation Centre (STIC), CUSAT, for their assistance in the characterization studies.

- Finishya Francis, Athira T V, Amritha Lakshmi M S

Contents

Chapter 1

Introduction

1.1 ENVIRONMENTAL POLLUTION AND GLOBAL CHALLENGES

Environmental pollution represents one of the most pressing global challenges of the 21st century, with contaminants from industrial, agricultural, and urban activities severely degrading the quality of air, water, and soil. Conventional remediation technologies often suffer from limitations, including low efficiency, high energy consumption, and the generation of secondary waste. In this context, nanotechnology has emerged as a transformative frontier, offering innovative solutions due to the unique physicochemical properties of nanomaterials, such as high surface area, enhanced reactivity, and tunable surface chemistry.

The world is on the edge of a major environmental calamity that will cost us our fortune. The current state of the present environment is forever deteriorating. Environmental issues are piling up across the globe, and we have to behave as if it were an emergency on our planet. We have to gain a new perspective and approach calamities beforehand with new concepts and strategies, and with our full awareness and seriousness. Pollution in nature, such as in air, water, and soil, takes millions of years to eradicate. Industry and automobile exhaust emissions are the main contributing factors to most of the environmental pollution. In the face of mounting global environmental challenges, industrial effluent—particularly from the textile, pharmaceutical, and printing sectors—poses a critical threat to water security and ecosystem health. This wastewater is notoriously laden

with persistent organic dyes, which are toxic, mutagenic, and resistant to natural degradation, alongside pathogenic microorganisms that jeopardise public health. Conventional remediation techniques often prove inadequate, being either inefficient, energy-intensive, or generating secondary pollutants, thereby necessitating the development of advanced, sustainable treatment technologies.

1.2 NANOMATERIALS FOR ENVIRONMENT REMEDIATION

Nanomaterials have emerged as a revolutionary platform for environmental remediation, offering high reactivity and multifunctionality.

Inadequacy of conventional methods and materials used in water remediation in eradicating organic, inorganic, and microbial contaminants has encouraged the research community to pursue nanotechnological aids for environmental needs. Nanotechnology is an emerging science that could be used in different fields. Nanomaterials have major benefits over bulk materials due to their larger surface area, greater reactivity, and therefore improved performance. Nanoremediation is an effective, rapid, and efficient technology to deal with persistent compounds such as pesticides, chlorinated solvents, halogenated chemicals, or heavy metals. Furthermore, nanoremediation is a sustainable alternative to eliminate emerging pollutants such as pharmaceuticals or personal care products. Nanomaterials enriched with tunable surface functionalities, excellent structural stability, high adsorption capacities, improved selectivity and specificity, enhanced biodegradability, and reusability of synthesised materials have been tried for environmental pollution mitigation. The environmental fate and toxicity of nanomaterials need to be considered for their use in abatement and remediation of environmental pollution. The success of the techniques in field conditions is a factor of

interdisciplinary works, which need successful collaboration of chemistry, material science, geology and biosciences.

1.3 CRYSTAL STRUCTURE OF ZnO

Zinc oxide (ZnO) crystallizes in a hexagonal wurtzite structure (space group $P6_3mc$), characterized by lattice parameters of a = 0.3296 nm and c = 0.52065 nm. Its atomic arrangement consists of alternating planes of tetrahedrally coordinated Zn^{2+} and O^{2-} ions stacked along the c-axis. This tetrahedral geometry results in a non-centrosymmetric structure, which is the origin of the piezoelectric and pyroelectric properties of ZnO.

A key feature of this structure is the presence of polar surfaces, most notably the basal planes. The stacking sequence creates positively charged Zn-terminated (0001) and negatively charged O-terminated (0001) surfaces, leading to a spontaneous dipole moment and polarization along the c-axis. Unlike most polar surfaces, which undergo reconstruction to stabilize, the ZnO ± (0001) surfaces remain remarkably stable and atomically flat—a subject of significant interest in surface science. Other common crystallographic facets in ZnO are the non-polar {2110} and {0110} families, which possess lower surface energy than the polar basal planes.

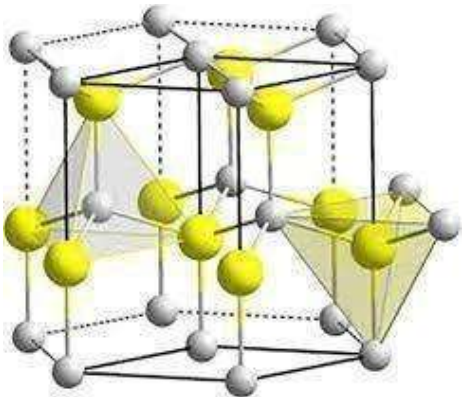

Fig1.1 Wurtzite crystal sturcture of ZnO

1.4 ENVIRONMENT REMEDIATION OF ZnO

ZnO also has the potential to photocatalytically degrade dyes. Human exposure to dyes over a significant amount of time can lead to harmful health conditions. Reactive dyes can cause respiratory sensitisation conditions, whereas vat dyes and azo dyes are associated with skin irritation. Azo dyes exhibit carcinogenic consequences and also impact the aquatic ecosystem, water–gas solubility, and transparency of water. Besides, azo derivatives like aromatic amines lead to blindness, chemosis and so forth, adverse conditions. The wastewater from textile industries contains metals like Copper, Chromium, etc., causing haemorrhages, skin ulcers and so on. The toxicity of dyes impacts soil microorganisms' death and subsequently affects agricultural yield. Therefore, to overcome these aforesaid adverse effects of dyes and provide a non-toxic environment for humans and the aquatic ecosystem, it is important to focus on the degradation of dyes. No particular technique is suitable for every type of dye degradation; thus, various methods are employed, namely oxidation, anaerobic degradation and coagulation.

1.5 MXENES: A NEW CLASS OF 2D MATERIALS

In 2011, researchers from Drexel University discovered a new class of inorganic compounds with a two-dimensional structure, which aroused great interest among scientists from all over the world. These unusual 2D materials were called MXenes. The family of MXenes consists of carbides, nitrides, or carbonitrides of transition metals. They are two- dimensional nanolayers with a thickness of several atoms and a planar size in the order of several micrometers. MXene materials have a wide range of unique properties that make them attractive and suitable for a variety of applications. For example, they have a large specific surface

area and high mechanical, electronic, and physicochemical properties, as well as excellent biocompatibility.

1.6 STRUCTURE AND PROPERTIES OF MXENES, SIGNIFICANT APPLICATIONS

The intrinsic structure consists of atomic layers of transition metals (M) interleaved with carbon/nitrogen (X) in a close-packed arrangement. A defining structural feature is that the M atoms at the surface are not saturated but are terminated by the 'T_x' functional groups. These terminations originate from the etching environment (e.g., F^-, OH^-, H_2O and are crucial; they dictate MXene's electronic properties, hydrophilicity, chemical stability, and interlayer spacing. This tunable surface chemistry is a primary reason for MXene's versatility in applications ranging from energy storage to catalysis.

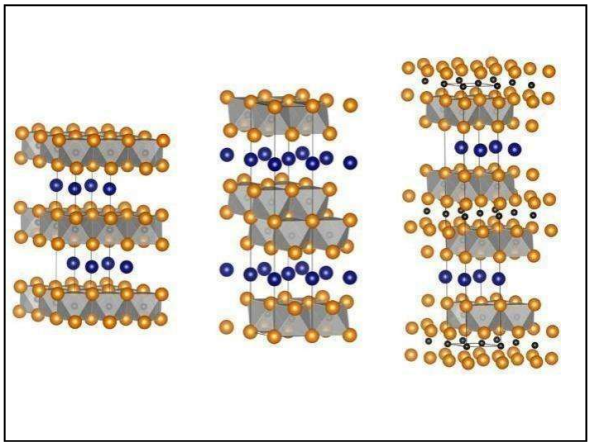

Fig1.2 Layered crystal structure of MXene

Metallic Conductivity: Applications like electrochemical sensing and energy storage (such as batteries and supercapacitors) depend heavily on metallic conductivity. Efficient electron transfer, which is necessary for quick signal transduction and energy transport in devices used for

environmental monitoring or renewable energy generation, is made possible by high conductivity.

Hydrophilicity: These materials' strong affinity for water facilitates their efficient interaction with contaminants in aqueous environments. This characteristic increases the contact area between the active material surface and waterborne contaminants and improves material dispersion in water treatment systems, which increases the effectiveness of remediation or sensing.

Surface Functional Groups: The presence of specific chemical groups (e.g., hydroxyl, carboxyl, amine) on the surface allows for tailored interactions with target analytes or pollutants. These groups provide active sites for chemical reactions or selective binding, which is crucial for specific and sensitive environmental detection or catalytic degradation of harmful substances.

Tunable Surface Chemistry: The ability to modify the surface chemistry allows researchers and engineers to optimize the material for specific environmental challenges. This tunability enables the precise control of properties like adsorption capacity, selectivity, and catalytic activity, making the materials versatile for a wide range of applications from water purification to gas sensing.

Compatibility with Semiconductors: This characteristic is vital in photoelectrochemical applications, such as solar energy conversion and photocatalytic degradation of pollutants. By integrating metallic materials with semiconductors, hybrid systems can be created that harness light energy more efficiently, leveraging the unique electronic properties of both components to enhance performance and stability.

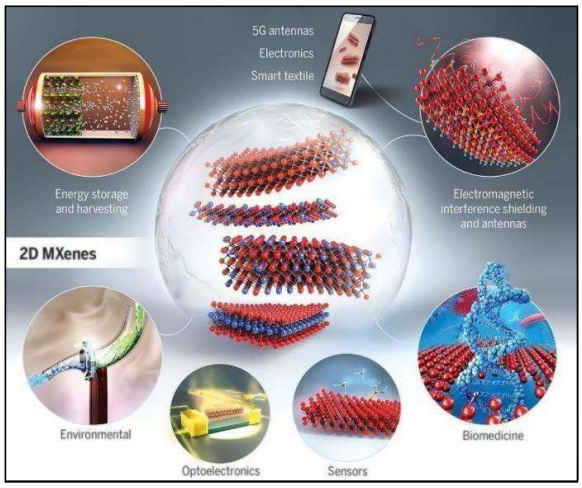

Fiq1.3 Application of 2D MXene materials

1.7 METHOD OF MXENE SYNTHESIS

MXenes are derived from the etching and exfoliation of the original hexagonally layered MAX phase (ternary transition metal carbides, carbonitrides and nitrides, where M, A and X refer to early transition metal (Cr, Nb, Ti, V, etc.), element from groups (e.g., Al, As, Cd, P, etc.) and carbon/nitrogen, respectively.

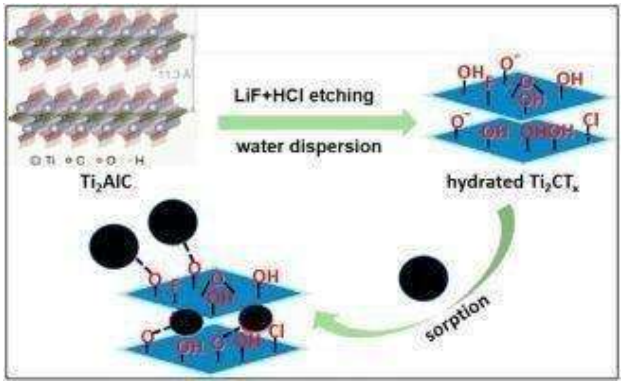

Fig1.4 Synthesis of MXene by LiF+HCl etching of MAX phase

Wet-chemical etching is the most common method to make MXenes and hydrofluoric acid was the first etchant used to make MXenes. It is found that F− anion is vital in the etching process. Thus, fluoride salt mixed with hydrochloric acid was also used to make MXenes. The wet-chemical

etching process for MXene synthesis is affected by environmental factors, such as temperature, pressure, and so on. Thus, by controlling these factors, more etching methods, such as hydrothermal etching and electrochemical etching, were used to synthesise MXenes effectively. Besides wet- chemical etching in aqueous solution, molten salt etching is also an important method to make MXenes with more terminations. The experimental conditions of the alkali-based etching are quite harsh (27.5 M NaOH, 270 °C in an autoclave), making it difficult to scale up. The molten salt method has only been used to produce Ti_4N_3 so far, requires high temperature (550 °C), fluoride 19 salts (lithium, sodium and potassium fluorides), and the yields are quite low.

After etching, the selectively dissolved atomic layers are replaced by various terminations, and the resulting material consists of $M_{n+1}X_nT_z$ multilayers (MLs) held together by hydrogen and/or van der Waals bonds. Single layers can then be exfoliated, or delaminated, into aqueous colloidal suspensions. Here, methods typically used to obtain other 2D materials are used: intercalation with large organic molecules, intercalation with cations, shaking, and/or sonication.

1.8 COMPARATIVE OVERVIEW OF ZnO/MXENE WITH ZnO/GRAPHENE, ZnO/rGO

Graphene and MXenes have emerged as promising materials for gas sensing applications due to their unique properties and superior performance. This review focuses on the fabrication techniques, applications, and sensing mechanisms of graphene and MXene-based composites in gas sensing. Gas sensors play a crucial role in various fields, including healthcare, environmental monitoring, and industrial safety, for detecting and monitoring gases such as Hydrogen Sulfide

(H_2S), Nitrogen Dioxide (NO_2), and Ammonia (NH_3). Conventional metal oxides such as Tin Oxide (SnO_2) and Zinc Oxide (ZnO) have been widely used, but Graphene and MXenes offer enhanced sensitivity, selectivity, and response times. Graphene-based sensors can detect low concentrations of gases like H_2S and NH_3, while functionalization can improve their gas-specific selectivity. MXenes, a new class of two-dimensional materials, exhibit high electrical conductivity and tunable surface chemistry, making them suitable for selective and sensitive detection of various gases, including VOCs and humidity. Other materials, such as metal-organic frameworks (MOFs) and conducting polymers, have also shown potential in gas sensing applications, which may be doped into graphene and MXene layers to improve the sensitivity of the sensors.

ZnO–MXene hybrids represent a promising and emerging class of nanohybrid materials that offer several potential advantages over the more established ZnO–graphene and ZnO–rGO composites. While ZnO–graphene/rGO systems are widely studied and valued for their excellent charge separation, enhanced visible-light absorption, and proven photocatalytic performance in dye degradation and hydrogen evolution, ZnO–MXene hybrids introduce unique benefits derived from the intrinsic properties of MXenes. Specifically, MXenes generally exhibit higher electrical conductivity—often metallic—which can facilitate even more efficient electron transfer compared to semiconducting graphene derivatives. Furthermore, MXenes possess tunable surface terminations (such as –O, –OH, –F) that enable stronger and more versatile interfacial bonding with ZnO, potentially leading to improved structural integration and charge-carrier dynamics. Another distinctive advantage is the photothermal effect inherent to many MXenes, which can augment photocatalytic activity under Near-Infrared (NIR) irradiation—a feature not

typically associated with graphene or rGO. Additionally, MXenes offer superior mechanical robustness and a richer surface chemistry, broadening their applicability into areas such as energy storage, biosensing, and photothermal therapy. However, it is important to note that ZnO–MXene hybrids are less mature in terms of synthesis protocols, face challenges related to oxidative stability in aqueous environments, and currently lack the extensive optimisation and morphological control seen in ZnO–graphene/rGO systems. Despite these hurdles, the enhanced conductivity, multifunctional surface properties, and photothermal capabilities position ZnO–MXene hybrids as a potentially superior alternative for next-generation photocatalytic, energy storage, and biomedical applications, provided that stability and scalable synthesis are effectively addressed.

MXenes exhibit a notable photothermal capability, a property not emphasised in the graphene-based studies, which could enable photocatalytic activity under near-infrared (NIR) light, extending the useful spectral range. While the ZnO–Graphene/rGO systems benefit from mature, scalable synthesis methods and extensive morphological control, the ZnO–MXene hybrid is less developed and faces stability challenges (such as aqueous oxidation) and more complex synthesis involving HF etching. Nevertheless, the superior conductivity, mechanically robust layered structure, and versatile surface functionalization of MXenes suggest that ZnO–MXene hybrids could outperform their graphene counterparts in applications requiring high electrical transport, photothermal enhancement, or multifunctional surface interactions, particularly in advanced energy storage, sensing, and biomedical applications, provided that their stability and synthesis are optimised in future research.

1.9 REPORTED ZnO/MXene ARCHITECTURE STRATEGIES

ZnO/MXene architecture strategies focus on creating hybrid composite materials that leverage the high conductivity of MXenes and the semiconducting properties/structural advantages of ZnO to enhance performance in applications like photocatalysis, energy storage, and sensing. Key architectural strategies and synthesis methods include:

1.9.1 Nanoparticle Decoration (0D/2D Architecture)

This common strategy involves decorating the surface of 2D MXene nanosheets with zero-dimensional (0D) ZnO quantum dots or nanoparticles. The primary goal is to prevent the restacking of MXene layers, increase the specific surface area, and provide a large number of active sites.

1.9.2 Hierarchical Nanorod/Microrod Growth (1D/2D Architecture)

This strategy involves growing one-dimensional (1D) ZnO nanorods or microrods, often using the MXene as a substrate. The major goal is to create a well-defined hierarchical structure with enhanced surface area, improved charge transfer efficiency, and structural integrity.

1.9.3 Three-Dimensional (3D) Architectures

These strategies involve creating macrostructures to exploit the porous nature and conductivity of MXene while incorporating ZnO. The primary goal is to reduce local current density, prevent MXene restacking in thick electrodes, increase active sites, and facilitate rapid ion diffusion in applications such as zinc-ion batteries.

2D transition metal carbides and/or nitrides (MXenes), by virtue of high electrical conductivity, abundant surface functional groups and excellent dispersion in various solvents, are attracting increasing attention and showing competitive performance in energy storage and conversion applications. However, like other 2D materials, MXene nanosheets are inclined to stack together via van der Waals interactions, which leads to a limited number of active sites, sluggish ionic kinetics, and finally ordinary performance of MXene materials/devices. Constructing 2D MXene nanosheets into 3D architectures has been proven to be an effective strategy to reduce restacking, thus providing a larger specific surface area, higher porosity, and shorter ion and mass transport distance over normal 1D and 2D structures. In this review, the commonly used strategies for manufacturing 3D MXene architectures (3D MXenes and 3D MXene- based composites) are summarised, such as template, assembly, 3D printing, and other methods. Special attention is also given to the structure–property relationships of 3D MXene architectures and their applications in electrochemical energy storage and conversion, including supercapacitors, rechargeable batteries, and electrocatalysis.

1.10 CHALLENGES AND KNOWLEDGE GAPS

Our project, which successfully demonstrated the practical synthesis of ZnO from $Zn(OH)_2$ and its hybridisation with HF-etched MXene, directly highlighted several critical knowledge gaps and persistent challenges in the field. The most immediate and significant challenge is the hazardous synthesis of MXene itself. The reliance on concentrated Hydrofluoric Acid (HF) for etching—a necessary step to produce the MXene nanosheets used in our hybrid—presents severe safety risks, as HF is highly toxic and carcinogenic. This makes the preparation of

MXene difficult and conflicts with the principles of green chemistry, posing a major barrier to commercial application. Furthermore, once synthesised, the environmental instability of MXenes becomes a key concern; the sheets are prone to oxidation, especially in aqueous photocatalytic environments, which can degrade the hybrid's performance over time—a challenge less prominent in stable ZnO-graphene composites. From a fundamental perspective, the precise nature of the interface between our solution-grown ZnO and the terminated MXene surface (Ti–O, –OH, etc.) is not fully understood. While ZnO-rGO bonds are well-studied, optimising the synergistic charge transfer in our ZnO-MXene hybrid remains partially empirical. Bridging these gaps requires future work focused on developing safer, non-HF etching methods, formulating strategies to passivate MXene against oxidation, and employing advanced characterisation to decipher the interfacial chemistry that dictates the hybrid's enhanced properties.

1.11 PROJECT OBJECTIVES

The core objective of this project is to successfully synthesise, characterise, and evaluate a novel ZnO–Mo_2TiC_2 MXene nanohybrid through a structured three-phase approach. The first phase is synthesising zinc oxide (ZnO) nanoparticles via a controlled chemical method, and the second, developing a reliable procedure to combine the synthesised ZnO with MXene (Mo_2TiC_2) to create an integrated hybrid material. Characterisation and Analysis involves a detailed examination of the hybrid's structural, morphological, and chemical properties using advanced techniques, including X-Ray Diffraction (XRD) for phase identification, Fourier-Transform Infrared Spectroscopy (FTIR) for

functional group analysis, and Scanning Electron Microscopy (SEM) for morphological and topographical study. Finally, Application Exploration aims to investigate the potential applications of the prepared nanohybrid, particularly in areas such as photocatalytic environmental remediation and antibacterial activity, to validate its functional performance and multifunctional potential.

Chapter 2

Materials and Methods

This chapter gives a brief description of the materials and experimental procedures adopted for the present investigation.

2.1 ZINC OXIDE SYNTHESIS

2.1.1 Chemicals Required

i. Zinc Acetate Dihydrate [$Zn(CH_3COO)_2.2H_2O$] – 1.728g

ii. CTAB (Cetyltrimethyl Ammonium Bromide) – 0.05g

iii. 1% Acetic Acid [CH_3COOH] (1mL Glacial Acetic Acid + 99mL distilled water)

iv. NaOH Pellets - 7 or 8 pellets

All chemicals are obtained from the college laboratory, St. Teresa's College (Autonomous), Ernakulam

2.1.2 Apparatus Required

i. Magnetic stirrer

ii. Mortar and Pestle

2.1.3 Procedure

The initial steps involve dissolving 0.05g CTAB in 1% Acetic Acid. To this, 1.728g Zinc Acetate Dihydrate. It is then kept for continuous stirring in a magnetic stirrer for 3 hours. Precipitation is performed by

adding water-dissolved NaOH pellets to the stirred mixture dropwise. Stirring is continued for an additional 1 hour after complete precipitation. Finally, Post processing method is performed, where the precipitate formed is washed and centrifuged. It is oven- dried at a temperature of 60 °C – 80 °C for 4 hours. The dried mixture is further calcinated at 450 °C for 4 hours in a Muffle furnace. The dried flakes of ZnO are powdered using a mortar and pestle.

Fig2.1 Reaction mixture of ZnO

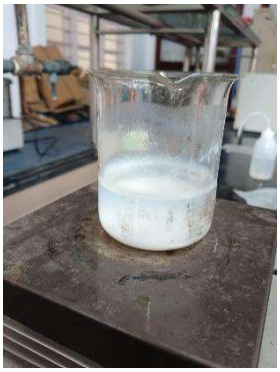

Fig2.2 ZnO precipitate

Fig2.3 ZnO sample for analysis

2.2 SYNTHESIS OF MXENE NANOPARTICLES

2.2.1 Chemicals Required

i. Mo_2TiAlC_2 (MAX Phase) – 1g

ii. HF Acid (40%) – 25mL

2.2.2 Apparatus Required

i. Ultrasonicator

2.2.3 Procedure

The synthesis of the Mo_2TiAlC_2 MXene was carried out via the selective etching of the Aluminium (Al) layer from the Mo_2TiAlC_2 MAX phase precursor. In a typical procedure, 1 g of Mo_2TiAlC_2 powder was slowly added to 25 mL of 40% hydrofluoric acid (HF) under constant stirring. To manage the exothermic nature of the initial reaction, the process was maintained under ice-bath control. The mixture was subsequently heated to 55°C and stirred for 24 hours, followed by an additional 48 hours of stirring at room temperature to ensure complete etching.

2.3 ZnO-Mo_2TiC_2 HYBRID SYNTHESIS

2.3.1 Chemicals Required

i. Mo_2TiAlC_2 MXene – 25mg

ii. Distilled Water – 99mL

iii. Zinc Acetate Dihydrate [$Zn(CH_3COO)_2.\ 2H_2O$] – 1.728g

iv. CTAB (Cetyltrimethyl Ammonium Bromide) – 0.05g

v. Glacial Acetic Acid – 1mL

vi. NaOH Pellets

2.3.2 Apparatus Required

i. Magnetic Stirrer

ii. Ultrasonicator

iii. Mortar and Pestle

2.3.3 Procedure

The ZnO–MXene hybrid nanocomposite was synthesised via an in situ precipitation and calcination method. Initially, 25 mg of MXene was dispersed in 99 mL of deionised water and ultrasonicated for 30 minutes at room temperature to obtain a homogeneous suspension. Subsequently, 1.728 g of zinc acetate dihydrate, 0.05 g of CTAB, and 1 mL of acetic acid were added to the MXene dispersion, and the mixture was stirred continuously until a clear and uniform precursor solution was formed. Aqueous NaOH solution was then added dropwise under constant stirring until precipitation occurred, followed by further stirring for 1 hour to ensure complete formation and deposition of Zinc hydroxide on the MXene surface. The resulting suspension was allowed to settle, and the precipitate was collected by decantation and washed several times with deionised water to remove impurities. The washed product was dried either overnight at 60°C or at 80 °C for 4 hours and subsequently calcined in a muffle furnace at 450°C for 2 hours. During calcination, Zinc hydroxide was converted into ZnO nanoparticles, which anchored onto the MXene sheets, yielding the final ZnO– MXene hybrid nanocomposite.

Fig2.4 Collected precipitate of ZnO MXene nanohybrid

Fig2.5 Dispersion process of ZnO MXene nanohybrid

Fig2.6 Ultrasonication of ZnO MXene nanohybrid

APPLICATION STUDY

2.4 DYE ADSORPTION

2.4.1 Chemicals Required

i. 50mg of the synthesised substance (ZnO Nanocrystals and ZnO-Mo_2TiC_2 Nanohybrid)

ii. 1mg of the cationic (Methylene Blue) and anionic (Rhodamine B) each.

2.4.2 Procedure

A 20 parts per million (ppm) dye solution was prepared for adsorption experiments by dissolving 1 mg of either Methylene Blue (cationic) or Rhodamine B (anionic) dye in 50 mL of distilled water. In separate trials, 50 mg of the synthesised adsorbent—either pure ZnO or the ZnO-MXene hybrid—was introduced into 50 mL of the dye solution. The mixture was then subjected to continuous magnetic stirring in the dark to minimise photodegradation interference.

Samples for analysis were extracted at defined time intervals to monitor the adsorption kinetics. An initial 10 mL aliquot was collected at t = 0 minutes (immediately before stirring). Subsequently, 10 mL samples were withdrawn at 10- minute intervals for the first hour. A final sample was collected after 24 hours of continuous stirring. Immediately after collection, each aliquot was centrifuged to separate the adsorbent particles. The resultant supernatant was carefully pipetted, shielded from light using Aluminium foil to prevent dye degradation, and stored for analysis.

The concentration of residual dye in each centrifugate was determined using UV- Vis spectrophotometry. The adsorption capacity of each material (ZnO and ZnO- MXene hybrid) was calculated based on the decrease in dye concentration relative to the initial (t=0) sample, thereby evaluating the kinetics and efficiency of the adsorption process.

2.5 ANTIMICROBIAL ANALYSIS

The synthesised compounds, ZnO and ZnO- Mo_2TiC_2 are subjected to antimicrobial analysis. The bacteria used are E. Coli and Bacillus Cereus.

- **Preparation of Nutrient Media**

Nutrient broth was prepared by dissolving 1.3 gm of nutrient broth in 100 ml distilled water. Test tubes were filled with 5 ml of nutrient broth and were sterilized using an autoclave. Nutrient agar media was prepared by mixing 1.3gm of nutrient broth and 2gm of agar-agar in 100 ml distilled water. The media was autoclaved and 20 ml each poured into sterile petri plates under aseptic conditions.

- **Preparation of microbial cultures**

The test organisms (E. Coli, Bacillus Cereus) were inoculated into 5 ml of sterilised nutrient broth and kept for overnight incubation at 37°C.

- **Well diffusion Method**

A lawn culture of each bacterium was prepared using sterilised cotton swabs. A sterilised swab was dipped into the bacterial suspension and moved side to side from top to bottom, leaving no space uncovered. The plate was rotated to 90 degrees, and the procedure was repeated to coat the entire plate with bacteria. Once the lawn had been prepared, wells of 6 mm diameter were cut into agar plates using a sterile well cutter. The wells were labelled, and 20 µL of samples, ZnO and ZnO-Mo2TiC2 was loaded into the corresponding wells. The antibacterial activity of the samples was compared with standard antibiotics available. This plate was incubated at 37°C for 24 hrs. The radius of

each zone was measured using a standard ruler in centimetres. If the compound is effective against bacteria at a certain concentration, no colonies will grow. This is the zone of inhibition, which is a measure of the compound effectiveness; the larger the clear area around the well, the more effective the compound.

Chapter 3

Results and discussion

3.1 X-RAY DIFFRACTION

Figure 3.1 shows the X-Ray diffraction spectrum of synthesised ZnO Nanoparticles using Zinc Acetate Dihydrate and glacial acetic acid.

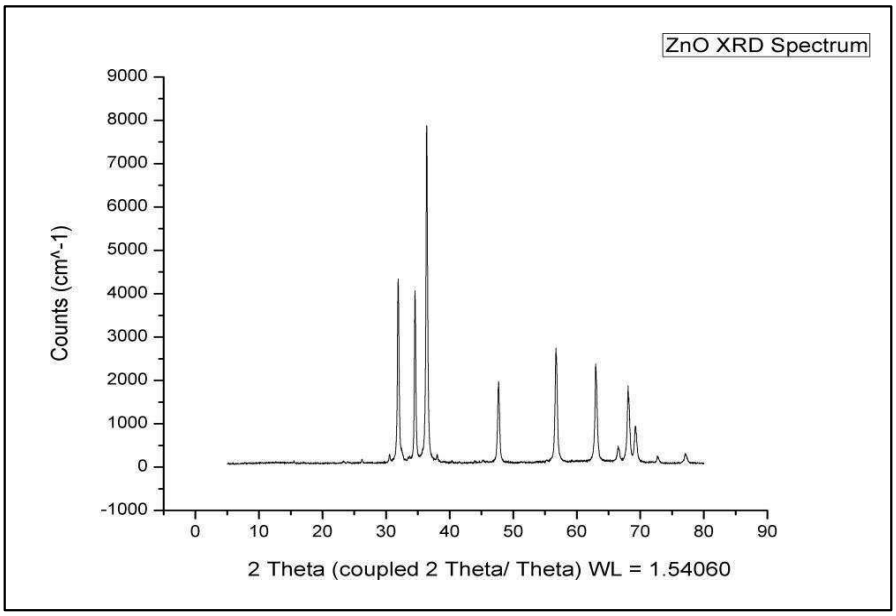

Fig 3.1 XRD Pattern of Synthesised ZnO Nanoparticles

Peaks are observed at 2θ ≈ 31.9°, 34.6° and 36.4° which correspond to the crystal planes (100), (002) and (101) respectively. Additional peaks at higher angles such as 37.9°, 40.3°, 44.0°, 47.7°, 56.7°, 62.9°, 66.5°, 68.0°, and 69.2° can be indexed to the planes (102), (110), (103), (112), (201), (202), (104), (203), and (210) respectively, which are also consistent with standard ZnO diffraction patterns.

Among the observed peaks, the (101) plane at $2\theta \approx 36.4°$ shows the highest intensity.

Figure 3.2 shows the X-Ray Diffraction spectrum of the synthesised ZnO-Mo_2TiC_2 Nanohybrid using Mo_2TiC_2 MXene and synthesised ZnO nanoparticles.

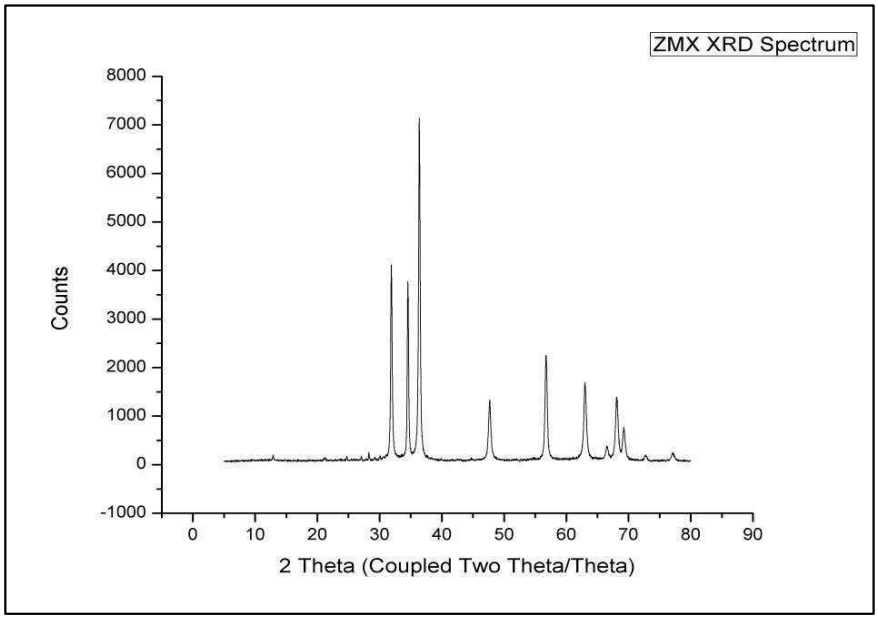

Fig 3.2 XRD Pattern of Synthesised ZnO-Mo_2TiC_2 Nanohybrid

Similar to the peaks of ZnO, the peaks of ZnO-Mo_2TiC_2 are found to be at $2\theta \approx 31.9°$, 34.6° and 36.4° which correspond to the crystal planes of ZnO (100), (002) and (101) respectively. Peaks are also observed at 47.7°, 56.7°, 62.9°, 66.5°, 68.0°, and 69.2°. However, the intensity of the peaks is lower when compared to those of pure ZnO nanoparticles. The presence of the low-angle (002) peak verifies the integration of the layered MXene (Mo_2TiC_2) phase.

3.2 FTIR CHARACTERIZATION

Figure 3.3 shows the FTIR Spectrum of the synthesized ZnO Nanoparticles using Zinc Acetate Dihydrate and Glacial Acetic Acid.

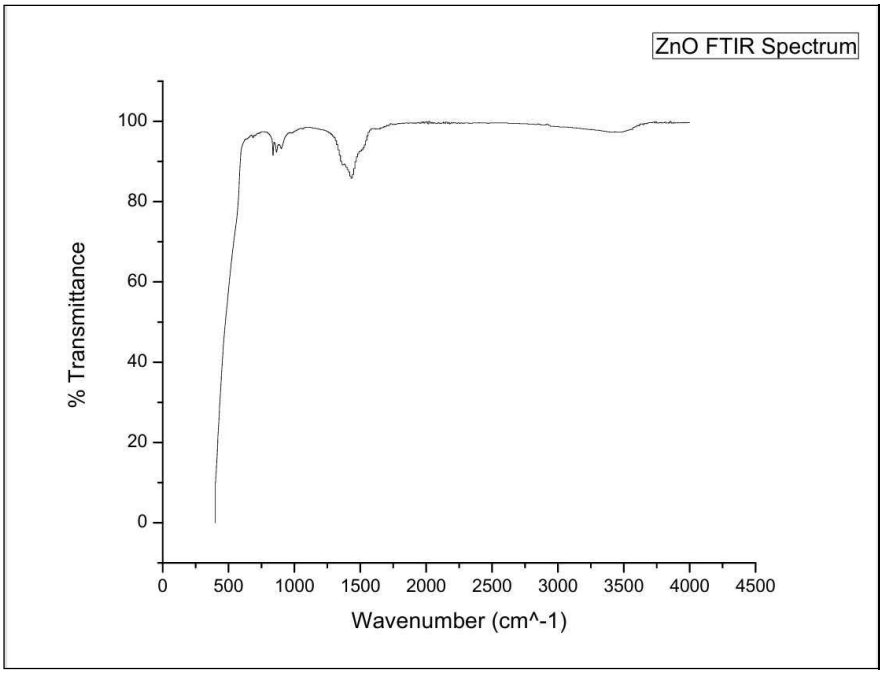

Fig 3.3 FTIR Spectrum of ZnO Synthesised Nanoparticles

The Spectrum also shows the highest peak at 400-600 cm^{-1} which corresponds to ZnO Stretching. A distinct peak is observed at 838.08 cm^{-1} which attributes to the C-H bending or other vibrations observed with organic residues. 1433.46 cm^{-1} shows a peak due to C=O stretching vibration.

Figure 3.4 shows the FTIR Spectrum of the synthesised ZnO-Mo_2TiC_2 Nanohybrid using Mo_2TiC_2 MXene and ZnO nanoparticles.

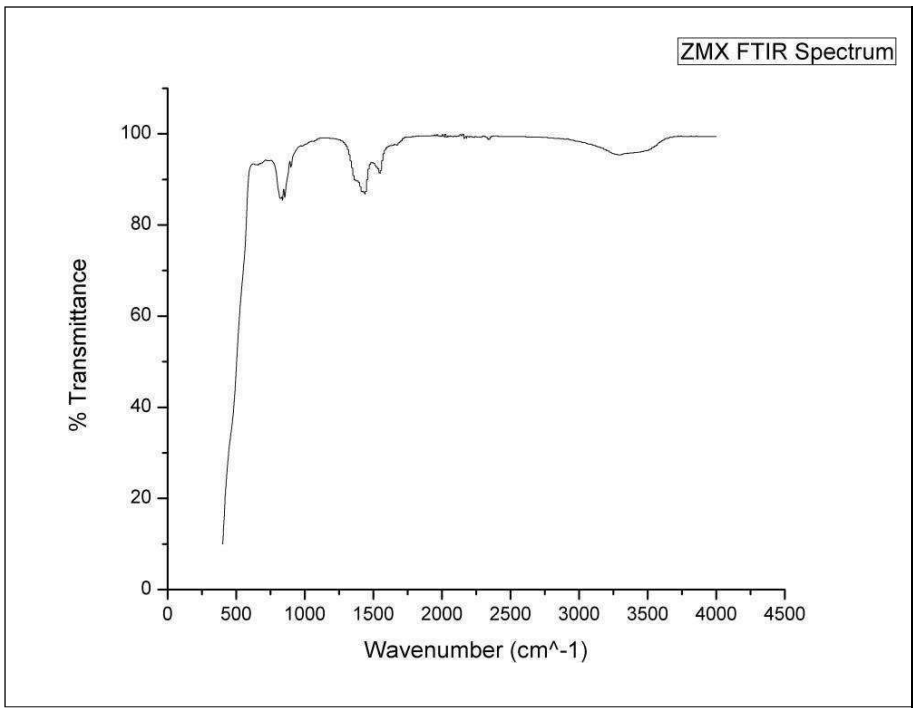

Fig 3.4 FTIR Spectrum of Synthesised ZnO-Mo_2TiC_2 Nanohybrid

The highest peak is found at 500cm^{-1} and 837.90cm^{-1} is due to Zn-O lattice vibration/stretching. The peak at 1439.90cm^{-1} shows symmetric stretching of Carboxylate (COO-), which originates from Zinc Acetate and Acetic Acid used. 1548 cm^{-1} also shows a peak due to the presence of adsorbed organic species, specifically Carboxylate (COO-) anion.

3.3 SEM ANALYSIS IMAGES

Fig 3.5, 3.6, 3.7, 3.8, 3.9 shows the SEM Analysis Images of synthesised ZnO-Mo_2TiC_2 Nanohybrid using Mo_2TiC_2 MXene and ZnO nanoparticles at different magnifications.

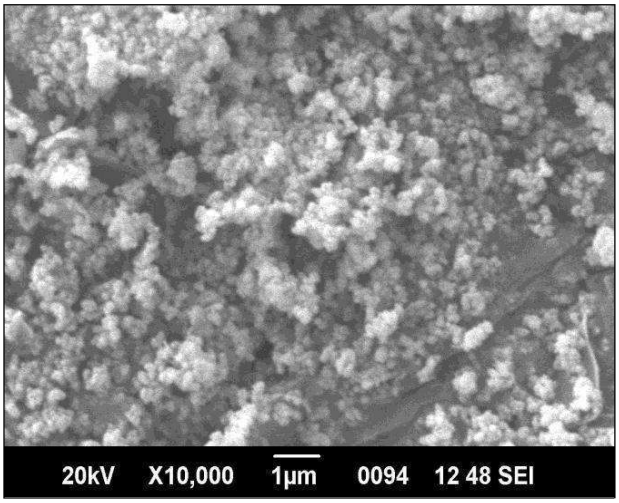

Fig 3.5 SEM Image of ZnO-Mo_2TiC_2 at 10,000X magnification

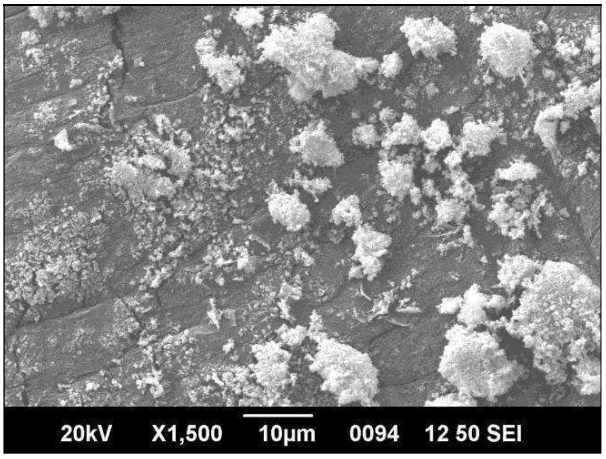

Fig 3.6 SEM Image of ZnO-Mo_2TiC_2 at 1,500X magnification

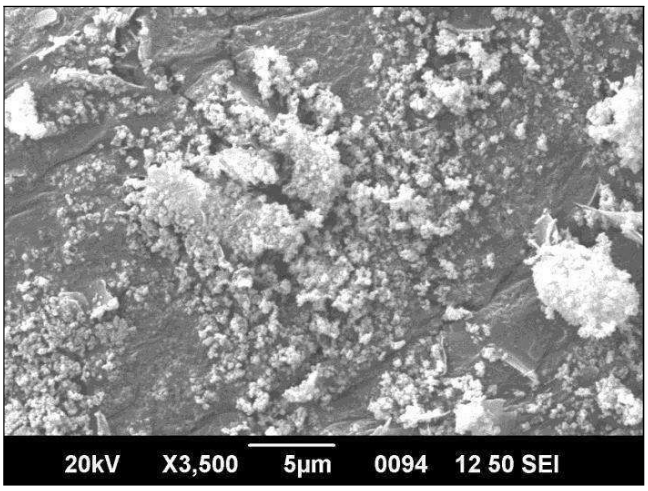

Fig 3.7 SEM Image of ZnO-Mo_2TiC_2 at 3,500X magnification

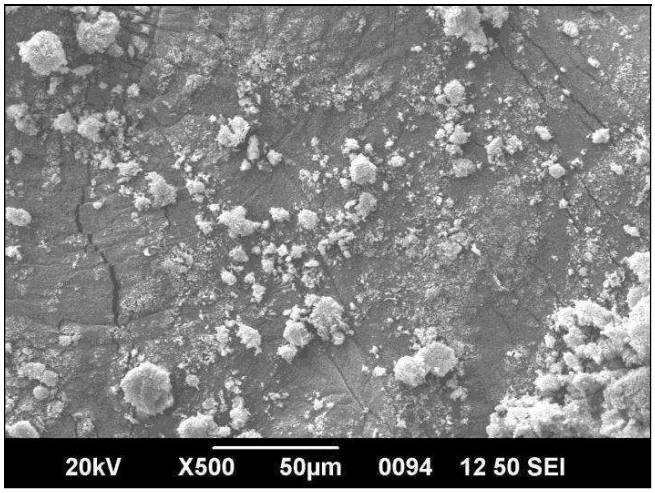

Fig 3.8 SEM Image of ZnO-Mo_2TiC_2 at 500X magnification

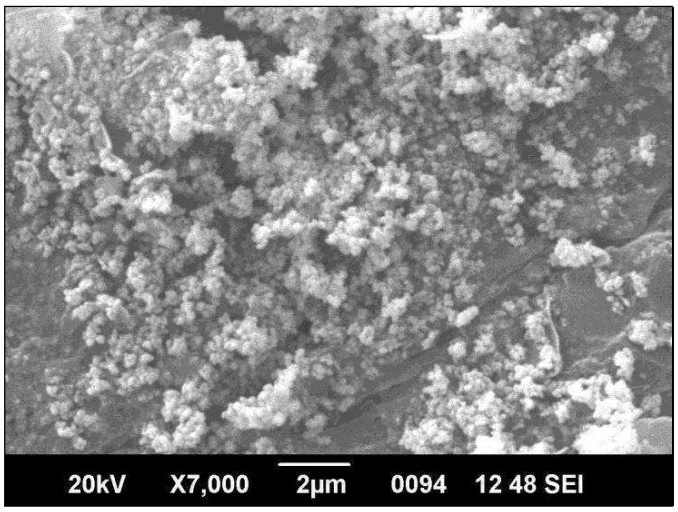

Fig 3.9 SEM Image of ZnO-Mo_2TiC_2 at 7,000X magnification

3.4 UV/VIS SPECTRUM OF DYE ADSORPTION

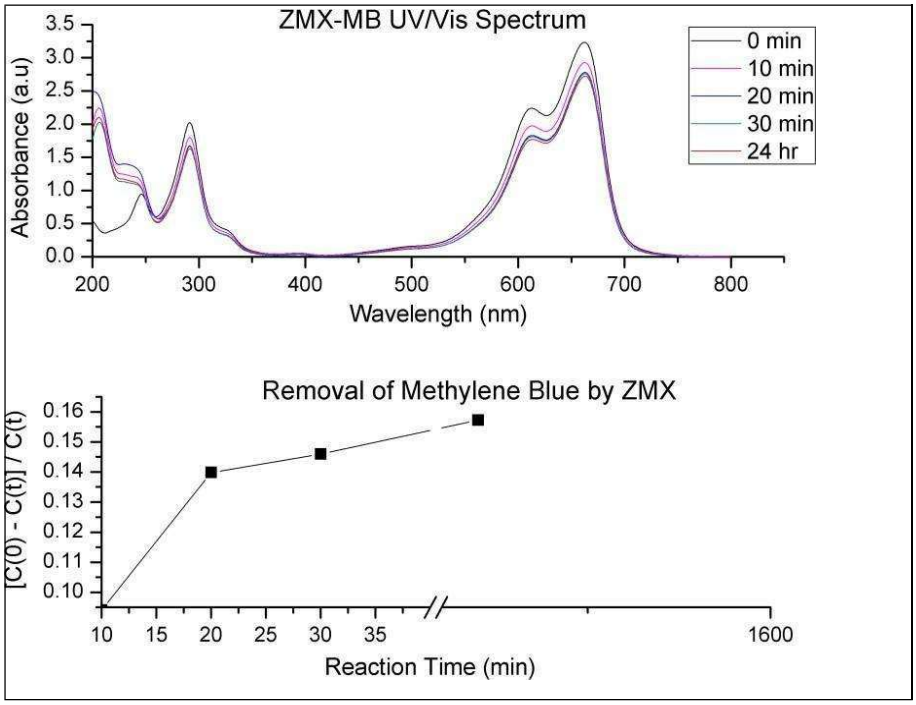

Fig 3.10 UV/VIS Spectrum and removal efficiency analysis of Synthesized ZMX Nanocomposite with Methylene blue dye

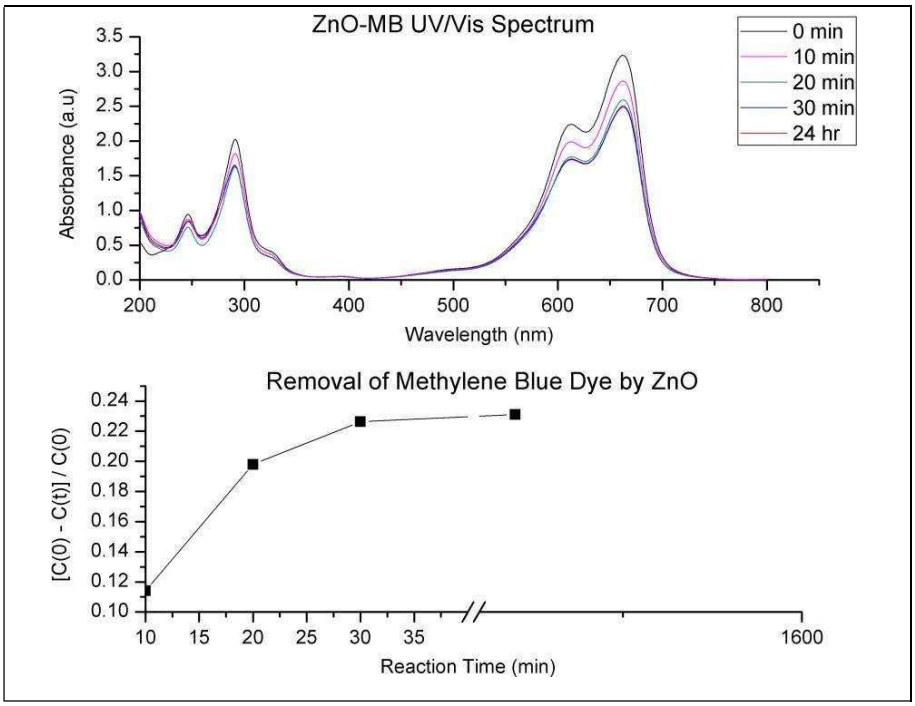

Fig 3.11 UV/VIS Spectrum and removal efficiency analysis of Synthesized ZnO with Methylene blue dye

For Methylene Blue (MB), both ZnO and the ZMX hybrid demonstrate rapid adsorption within the first 30 minutes, indicated by the sharp decrease in the characteristic absorption peak at approximately 664 nm. Due to the high surface area and presence of functional groups, ZnO- Mo_2TiC_2 shows a distinct dye adsorption profile. The removal of Methylene Blue shows a sharp increase with time.

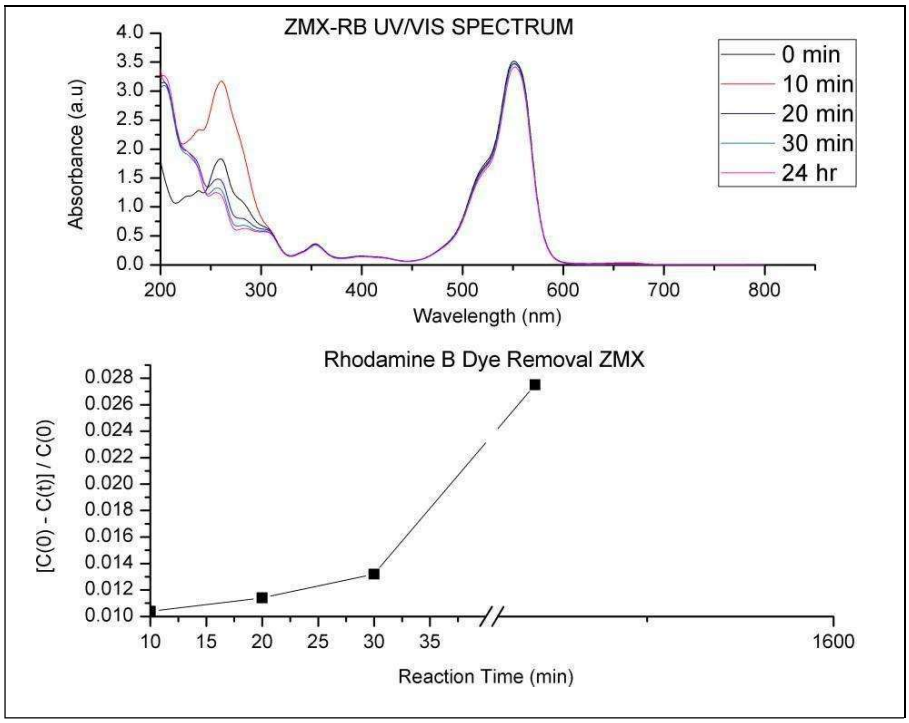

Fig 3.12 UV/VIS Spectrum and removal efficiency analysis of Synthesized ZMX Nanocomposite with Rhodamine B

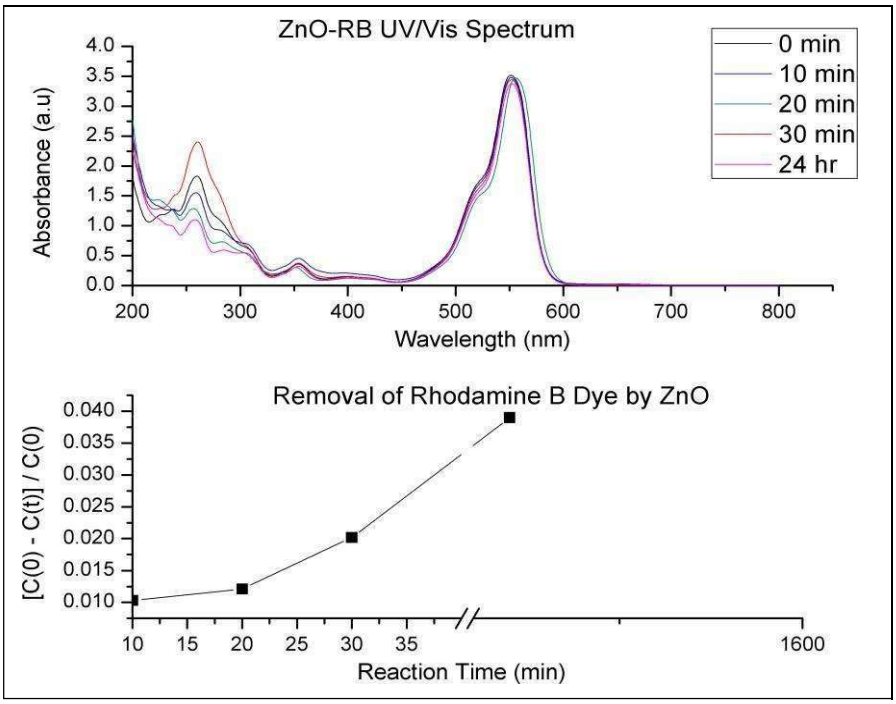

Fig 3.13 UV/VIS Spectrum and removal efficiency analysis of Synthesized ZnO with Rhodamine B

Rhodamine B (RB), in the UV-Vis spectra shows a peak at ~554 nm. This implies that the adsorption process is slower compared to MB for both materials. While ZnO shows a removal efficiency [C(0) - C(t)] / C(0)] reaching nearly 0.04 at the 24-hour mark, the ZMX hybrid exhibits a slightly lower removal value of approximately 0.028 for the same period.

The UV/Vis Spectra of the adsorbed dye, both Methylene Blue and Rhodamine B, are analyzed, and it is found that ZnO-Mo_2TiC_2 Hybrid shows more dye adsorption capacity than Pure ZnO nanoparticles due to its distinct structural properties. The graph shows a comparatively greater % of dye removal of both Methylene Blue and Rhodamine B for ZnO-MXene Hybrid than when its parent ZnO nanoparticles.

3.5 ANTIMICROBIAL ANALYSIS

Fig 3.15 Antimicrobial study of ZnO and ZnO-Mo_2TiC_2 with B.Cereus

Fig 3.16 Antimicrobial study of ZnO and ZnO-Mo_2TiC_2 with E. Coli

The fig 3.14 and 3.15 shows antimicrobial activity of ZnO and ZnO–MXene hybrid (ZMX) was evaluated against E coli and Bacillus cereus using the agar well diffusion method. Gentamicin (GEN 10) showed a clear, large inhibition zone, validating the experiment. ZnO and ZMX produced only small, vague zones, indicating low to moderate antibacterial activity, with no significant difference between them.

Chapter 4

Conclusions

Our research successfully synthesised ZnO nanoparticles and ZnO-Mo_2TiC_2 Nanohybrids. The structural, morphological and functional properties of the synthesized compound were also studied. The potential of the prepared material was validated through targeted application assessments.

Zinc Oxide nanoparticles were synthesised by chemical precipitation using Zinc Acetate Dihydrate. Mo_2TiC_2 MXene was also prepared by selective etching of the Aluminium layer from Mo_2TiAlC_2 MAX Phase. ZnO-Mo_2TiC_2 Nanohybrids were prepared similarly to the chemical precipitation of ZnO using Zinc Acetate Dihydrate, incorporating Mo_2TiAlC_2 with it. The MXene sheets were anchored to the surface of ZnO, as confirmed by the subsequent characterization.

The X-Ray Diffraction spectra of ZnO explained the hexagonal wurtzite structure of the compound, with associated changes and peaks in its MXene hybrid. FTIR Characterization of ZnO particles showed distinct peaks that illustrated Zn-O stretching, the presence of -OH and H-O-H bonds, which depict the presence of moisture . FTIR spectra

of ZnO-Mo_2TiC_2 Nanohybrid, similar to ZnO, showed distinct peaks illustrating Zn-O stretching vibrations, presence of more pronounced -OH peaks describing the enhanced hydrophilicity of the Nanohybrid. Additionally, several other peaks were also found, which correspond to the presence of Mo_2TiAlC_2 sheets anchored to the ZnO Nanoparticles. The SEM Analysis images also gave a three-dimensional representation of the synthesised hybrid.

The Dye adsorption capacity of the substance was also studied, and it was found that the adsorption power of ZnO- Mo_2TiAlC_2 was greater than that of ZnO Nanoparticles. The peaks of dye adsorption of Methylene Blue are observed at ~554nm, and that of Rhodamine B is observed at ~664nm. The absorbance of UV rays considerably decreases with an increase in stirring time.

In conclusion, the effective dye adsorption studies of the synthesized ZnO-Mo_2TiAlC_2 hybrid and its subsequent physical, structural and morphological properties make it an efficient agent in treating dye-polluted water bodies, creating an excellent tool in environmental remediation.

The antimicrobial activity of ZnO and ZnO–MXene hybrid (ZMX) was evaluated against Escherichia coli and Bacillus cereus using the agar well diffusion method. Both ZnO and ZMX samples showed only small and less distinct zones of inhibition, indicating low to moderate antibacterial activity under the tested conditions. The difference in activity between ZnO and ZMX was not highly significant from the observed plates.

The relatively low antibacterial effect may be due to factors such as insufficient sample concentration, limited diffusion of nanoparticles in the agar medium, or reduced generation of reactive oxygen species (ROS). Although the ZnO–MXene hybrid is expected to enhance antimicrobial performance due to increased surface area and improved interaction with bacterial cells, this enhancement was not strongly evident in the present study.

Overall, the results suggest that while the samples possess some antibacterial activity, further optimization (such as higher concentration or improved synthesis) is required to achieve significant antimicrobial efficiency.

References

1. Akhter, R., & Maktedar, S. S. (2023). MXenes: A comprehensive review of synthesis, properties, and progress in supercapacitor applications. *Journal of Materiomics*, *9*(6), 1196–1241. https://doi.org/10.1016/j.jmat.2023.08.011
2. Arjun, S., Krishna, A. B., Vamadevan, R., & Babu, J. S. (2024). Morphological, structural and electronic properties of zinc oxide nano structures deposited on ZnO substrate layer – A theoretical perspective. *Materials Today Communications*, *39*, 109231. https://doi.org/10.1016/j.mtcomm.2024.109231
3. Chauke, N. M., Mohlala, R. L., Ngqoloda, S., & Raphulu, M. C. (2024a). Harnessing visible light: enhancing TiO2 photocatalysis with photosensitizers for sustainable and efficient environmental solutions. *Frontiers in Chemical Engineering*, *6*. https://doi.org/10.3389/fceng.2024.1356021
4. Chauke, N. M., Mohlala, R. L., Ngqoloda, S., & Raphulu, M. C. (2024b). Harnessing visible light: enhancing TiO2 photocatalysis with photosensitizers for sustainable and efficient environmental solutions. *Frontiers in Chemical Engineering*, *6*. https://doi.org/10.3389/fceng.2024.1356021
5. Handore, K., Bhavsar, S., Horne, A., Chhattise, P., Mohite, K., Ambekar, J., Pande, N., & Chabukswar, V. (2014). Novel Green Route of Synthesis of ZnO Nanoparticles by Using Natural Biodegradable Polymer and Its Application as a Catalyst for Oxidation of Aldehydes. *Journal of Macromolecular Science, Part A*, *51*(12), 941–947. https://doi.org/10.1080/10601325.2014.967078
6. Kang, W., Jimeng, X., & Xitao, W. (2016). The effects of ZnO morphology on photocatalytic efficiency of ZnO/RGO nanocomposites32

Applied Surface Science, *360*, 270–275. https://doi.org/10.1016/j.apsusc.2015.10.190

7. Kumari, M. (2023). Role of nanomaterials in environmental remediation. In *Adsorption through Advanced Nanoscale Materials* (pp. 83–99). Elsevier. https://doi.org/10.1016/B978-0-443-18456-7.00005-5
8. Li, K., Liang, M., Wang, H., Wang, X., Huang, Y., Coelho, J., Pinilla, S., Zhang, Y., Qi, F., Nicolosi, V., & Xu, Y. (2020). 3D MXene Architectures for Efficient Energy Storage and Conversion. *Advanced Functional Materials*, *30*(47). https://doi.org/10.1002/adfm.202000842
9. Li, X., Bai, Y., Shi, X., Su, N., Nie, G., Zhang, R., Nie, H., & Ye, L. (2021). Applications of MXene ($Ti_3C_2T_x$) in photocatalysis: a review. *Materials Advances*, *2*(5), 1570–1594. https://doi.org/10.1039/D0MA00938E
10. Mahmood, T., & Baig, F. (2024). *A comparative study of ZnO, ZnO/GO and ZnO/RGO nanocomposites for the energy application.* https://doi.org/10.21203/rs.3.rs-4462456/v1
11. Padmanabhan, N. T., Gayathri, K., Thomas, R. M., & John, H. (2025). ZnO/Mo2TiC2 MXene nanohybrids for enhanced solar-driven photocatalytic degradation of tetracycline and organic pollutants in contaminated water. *Energy & Environmental Sustainability*, *1*(3), 100042. https://doi.org/10.1016/j.eesus.2025.100042
12. Pogorielov, M., Smyrnova, K., Kyrylenko, S., Gogotsi, O., Zahorodna, V., & Pogrebnjak, A. (2021). MXenes—A New Class of Two-Dimensional Materials: Structure, Properties and Potential Applications. *Nanomaterials*, *11*(12), 3412. https://doi.org/10.3390/nano11123412
13. Vaishag, P. V., & Noh, J.-S. (2024). A Comparative Review of Graphene and MXene-Based Composites towards Gas Sensing. *Molecules*, *29*(19), 4558. https://doi.org/10.3390/molecules29194558
14. Verger, L., Natu, V., Carey, M., & Barsoum, M. W. (2019). MXenes: An Introduction of Their Synthesis, Select Properties, and Applications.

Trends in Chemistry, *1*(7), 656–669. https://doi.org/10.1016/j.trechm.2019.04.006

15. Wang, Z. L. (2004). Zinc oxide nanostructures: growth, properties and applications. *Journal of Physics: Condensed Matter*, *16*(25), R829–R858. https://doi.org/10.1088/0953-8984/16/25/R01
16. Al-Arjan, W. S. (2022). Zinc Oxide Nanoparticles and Their Application in Adsorption of Toxic Dye from Aqueous Solution. Polymers, 14(15), 3086. https://doi.org/10.3390/polym14153086
17. Ali, M. A., Idris, M. R., & Quayum, M. E. (2013). Fabrication of ZnO nanoparticles by solution-combustion method for the photocatalytic degradation of organic dye. Journal of Nanostructure in Chemistry, 3(1), 36. https://doi.org/10.1186/2193-8865-3-36
18. Andrade-Guel, M., Cabello-Alvarado, C., Bartolo-Pérez, P., Medellin-Banda, D. I., Ávila-Orta, C. A., Cruz-Ortiz, B., Espinosa-Muñoz, A., & Cadenas Pliego, G. (2022). Surface modification of TiO 2 /ZnO nanoparticles by organic acids with enhanced methylene blue and rhodamine B dye adsorption properties. RSC Advances, 12(44), 28494–28504. https://doi.org/10.1039/D2RA04961A
19. Bilal, M., Khan, U., & Ihsanullah, I. (2023). MXenes: The emerging adsorbents for the removal of dyes from water. Journal of Molecular Liquids, 385, 122377. https://doi.org/10.1016/j.molliq.2023.122377
20. Hendrix, Y., Rauwel, E., Nagpal, K., Haddad, R., Estephan, E., Boissière, C., & Rauwel, P. (2023). Revealing the Dependency of Dye Adsorption and Photocatalytic Activity of ZnO Nanoparticles on Their Morphology and Defect States. Nanomaterials, 13(13), 1998. https://doi.org/10.3390/nano13131998
21. Jiang, W., Chen, X., Yan, X., Li, J., Xie, L., & Yu, Y. (2024). Adsorption studies of methylene blue on cation-modified graphene oxide and graphene oxide/MXene membranes. Colloids and Surfaces A:

Physicochemical and Engineering Aspects, 702, 135098. https://doi.org/10.1016/j.colsurfa.2024.135098

22. Kadhom, M., Kalash, K., & Al-Furaiji, M. (2022). Performance of 2D MXene as an adsorbent for malachite green removal. Chemosphere, 290, 133256. https://doi.org/10.1016/j.chemosphere.2021.133256
23. Kalpana, V. N., Kataru, B. A. S., Sravani, N., Vigneshwari, T., Panneerselvam, A., & Devi Rajeswari, V. (2018). Biosynthesis of zinc oxide nanoparticles using culture filtrates of Aspergillus niger: Antimicrobial textiles and dye degradation studies. OpenNano, 3, 48–55. https://doi.org/10.1016/j.onano.2018.06.001
24. Karim, Z. (2024). Laser-Ablation-Synthesized Ag/Zno-Dye Nanocomposite for Linear and Nonlinear Optical Applications. Nanomedicine & Nanotechnology Open Access, 9(1), 1–9. https://doi.org/10.23880/nnoa-16000284
25. Kataria, N., & Garg, V. K. (2017). Removal of Congo red and Brilliant green dyes from aqueous solution using flower shaped ZnO nanoparticles. Journal of Environmental Chemical Engineering, 5(6), 5420–5428. https://doi.org/10.1016/j.jece.2017.10.035
26. Manikandan, A. S., Renukadevi, K. B., Ravichandran, K., Rajkumar, P. v., & Boubaker, K. (2016). Enhanced photocatalytic, antibacterial and magnetic properties of ZnO nanopowders through lattice compatible cobalt doping. Journal of Materials Science: Materials in Electronics, 27(11), 11890–11901. https://doi.org/10.1007/s10854-016-5334-3
27. Najibikhah, P., Shayesteh, H., & Rahbar-Kelishami, A. (2025). Two-dimensional Ti3C2Tx MXene/MOF composite for enhanced methylene blue adsorption. Journal of Molecular Liquids, 429, 127627. https://doi.org/10.1016/j.molliq.2025.127627
28. Qu, J., Teng, D., Zhang, X., Yang, Q., Li, P., & Cao, Y. (2022). Preparation and regulation of two-dimensional Ti3C2Tx MXene for enhanced adsorption–photocatalytic degradation of organic dyes in

wastewater. Ceramics International, 48(10), 14451–14459. https://doi.org/10.1016/j.ceramint.2022.01.338

29. Samsuddin, A. F., Aziz, S. N. Q. A. A., & Pung, S.-Y. (2017). Loading effect of Ag/AgO on the photocatalytic performance of ZnO rods. Applied Physics A, 123(1), 101. https://doi.org/10.1007/s00339-016-0699-y
30. Yin, B., Zhang, S., Zhang, D., Jiao, Y., Liu, Y., Qu, F., & Wu, X. (2014). ZnO Film Photocatalysts. Journal of Nanomaterials, 2014(1). https://doi.org/10.1155/2014/186916